International Journal of Applied Pharmaceutics

ISSN- 0975-7058 Vol 18, Issue 2, 2026

Original Article

FORMULATION AND DEVELOPMENT OF GREEN-SYNTHESIZED ADAPALENE-CONJUGATED SILVER NANOPARTICLES INCORPORATED INTO *ALOE VERA* GEL FOR TOPICAL MANAGEMENT OF ACNE VULGARIS IN WOMEN

FARHAT FATIMA[1*], ASMA B. OMER[2], AHMED AL SAQR[1], MOHAMMED MUQTADER AHMED[1]

[1]Department of Pharmaceutics, College of Pharmacy, Prince Sattam Bin Abdulaziz University, Al-Kharj-11942, Saudi Arabia. [2]Department of Health Sciences, College of Health and Rehabilitation Sciences, Princess Nourah bint Abdulrahman University, P. O.-84428, Riyadh, Saudi Arabia

[*]Corresponding author: Farhat Fatima; [*]Email: f.soherwardi@gmail.com

Received: 13 Dec 2025, Revised and Accepted: 06 Feb 2026

ABSTRACT

Objective: This study aimed to improve acne treatment in women through the green synthesis of adapalene-conjugated silver nanoparticles using *Moringa oleifera* leaf extract, incorporated into an *aloe vera* gel.

Methods: The prepared adapalene-conjugated silver nanoparticles (ADN–AgNPs) were characterized for particle size, polydispersity index (PDI), and zeta potential (ζP) using dynamic light scattering, while physicochemical interactions were evaluated by Fourier transform infrared spectroscopy (FTIR), X-ray diffraction (XRD), Brunauer–Emmett–Teller (BET) surface area analysis, and scanning electron microscopy (SEM). Entrapment efficiency (EE) and drug loading (DL) were quantified spectrophotometrically. *In vitro* release and antimicrobial activity were also assessed.

Results: The optimized formulation exhibited a mean hydrodynamic particle size of 228.5 nm, a polydispersity index of 0.502, and a zeta potential of −24.5 mV, indicating nanoscale particles with moderately broad size distribution and adequate colloidal stability typical of phyto-mediated green synthesis. FTIR spectra showed characteristic peak shifts confirming successful adapalene conjugation onto phytochemical-capped silver nanoparticles. X-ray diffraction analysis confirmed the formation of crystalline face-centered cubic silver nanoparticles, while additional peaks were attributed to phytochemical capping components. BET analysis demonstrated a high specific surface area (88.29 m^2/g), while SEM micrographs showed quasi-spherical nanoparticles stabilized by phytochemical capping. The nanoparticles exhibited high entrapment efficiency (97.85%) and drug loading (48.92%). Incorporation into *aloe vera* gel produced a stable formulation with suitable pH, viscosity, spreadability, and uniform drug distribution. *In vitro* release studies showed significantly enhanced adapalene release (97.99±1.89% within 6 h), representing a 2.26-fold improvement over a marketed gel and following anomalous (non-Fickian) release kinetics governed by combined diffusion and polymer relaxation. Antimicrobial evaluation demonstrated strong inhibition against *Escherichia coli* (13±0.36 mm) and *Staphylococcus aureus* (16±0.14 mm), attributable to the collective contributions of silver nanoparticles, adapalene, and phytochemical constituents.

Conclusion: The developed ADN–AgNPs loaded *aloe vera* gel represents a promising eco-friendly, multifunctional topical delivery system offering enhanced drug release, antimicrobial efficacy, and therapeutic potential for acne management in women.

Keywords: Acne vulgaris, Adapalene, Silver nanoparticles, *Moringa oleifera*, *aloe vera* gel, Topical nanocarrier

DOI: https://dx.doi.org/10.22159/ijap.2026v18i2.57772 Journal homepage: https://innovareacademics.in/journals/index.php/ijap

INTRODUCTION

Acne vulgaris is one of the most prevalent chronic inflammatory skin disorders, affecting 85–90% of teenagers globally and more than 50% of adult women, with higher rates observed in certain ethnic groups. It remains a significant psychosocial burden, contributing to scarring, reduced self-esteem, and long-term therapeutic relapse. Because acne typically develops within the pilosebaceous units of the skin, topical preparations such as gels, creams, lotions, and ointments serve as the first-line treatment for mild to moderate cases [1]. These formulations act directly at the affected site, providing targeted, effective, and safe therapy with minimal systemic effects.

Adapalene (ADN) is a BCS class II drug that reflects low solubility and high permeability. The effectiveness of ADN is widely accepted and evidence-based in the treatment of acne, especially for women and teens [2]. Acne poses a significant psychosocial burden, particularly during adolescence. The problem with the conventional available creams and ointments is in their delivery systems, as the epidermal barrier limits drug delivery into deeper skin layers, thereby causing recurrence to happen frequently, leading to ineffectiveness of the therapy and non-compliance with the treatment [3].

ADN is a third-generation adamantine acid derivative that contains an adamantine group and a methoxyphenyl group, selectively binds nuclear retinoic-acid receptors (RAR-β/γ), is photostable, and has minimal systemic absorption compared to tretinoin. It acts by normalizing keratinocyte differentiation (anti-comedogenic/comedolytic) and down-regulating inflammatory pathways (e. g., AP-1, lipoxygenase activity, neutrophil chemotaxis), thereby being effective for treating acne [4]. Therapeutically used for acne vulgaris, photoaging, keratosis pilaris, and melasma, normally applied topically in the dose strengths of 0.1% and 0.3% [2].

As the ADN is classified in BCS-II, topical delivery deeper inside the skin is quite difficult; therefore, nanocarrier-based delivery systems represent a promising strategy to cross ADN through heterogeneous skin regions, combined with the silver ion concomitant to the antimicrobial activity of ADN [5].

Silver nanoparticles (AgNPs) not only improve dermal delivery but also provide additional antimicrobial activity, resulting in a combined antimicrobial effect with conjugated ADN for enhanced acne management. Besides, it acts as a stabilizer and protects the drug from photodegradation and oxidation, breaks down bacterial biofilms on follicles and skin surface, reducing treatment resistance, accelerates tissue regeneration and epithelial repair, and is useful for acne lesions and post-acne scars [6]. Physicochemical characteristics of AgNPs, such as having a large effective surface area, tunable size, and surface reactivity, make them suitable for topical drug delivery systems. Different methods of fabrication of AgNPs determine their particle size, stability, and biological activity. Among various synthesis approaches, green synthesis using plant extracts as reducing agents and stabilizers offers a safe, eco-friendly, and cost-effective method [7]. Chemical constituents of the plants-flavonoids, phenolics, terpenoids, and alkaloids-act as natural

reducing and capping agents, enabling the formation of stable nanosilver dispersions under experimental conditions [8]. Therefore, the green synthesis of AgNPs represents a promising approach for developing biocompatible therapeutic nanomaterials suitable for dermatological applications, including acne treatment [9]. The common ADN dose-related adverse effects are dryness, erythema, scaling, and stinging/burning; therefore, investigators plan to infuse the ADN-conjugated AgNPs into the formulated *aloe vera* gels, which have the multifunctional therapeutic benefits of promoting moisturization, anti-inflammatory, antimicrobial, and antioxidant effects, and enhancing drug permeation [10].

Nanocarrier-mediated topical delivery has emerged as a promising strategy to overcome the formidable barrier function of the stratum corneum. Nanoparticles with sizes below 500 nm are particularly advantageous for topical applications, as they preferentially accumulate within pilosebaceous units and hair follicles, which serve as natural shunt pathways bypassing the dense corneocyte–lipid matrix of the stratum corneum. In addition to size, surface chemistry plays a critical role in skin interaction [5]. Phytochemical capping derived from *Moringa oleifera* leaves provides bioactive functional groups such as polyphenols, flavonoids, and organic acids on the nanoparticle surface, which can enhance affinity toward follicular lipids and sebaceous secretions. These surface-associated phytochemicals may promote localized retention within follicles, modulate lipid packing within the stratum corneum, and facilitate sustained drug release at the pilosebaceous unit-the primary site of acne pathogenesis. Therefore, the combined effects of nanoscale dimensions and phyto-capped surface chemistry are expected to enhance follicular targeting and localized dermal delivery of adapalene, while minimizing systemic exposure.

This study hypothesizes that conjugating adapalene to green-synthesized AgNPs and incorporating them into *aloe vera* gel will create a multifunctional topical system with enhanced drug loading, improved dermal permeation, sustained release, and multifunctional antimicrobial effect compared with conventional formulations. The research aims to synthesize, characterize, and evaluate this ADN–AgNPs topical gel through physicochemical, pharmaceutical, release, and antimicrobial analyses for its potential application in acne management.

MATERIALS AND METHODS

Adapalene (ADN), an active pharmaceutical ingredient procured from Jazeera Pharmaceutical Industries, Riyadh. Silver nitrate ($AgNO_3$, analytical grade), purchased from Sigma-Aldrich (St. Louis, MO, USA). Fresh leaves of *Moringa oleifera* and *Aloe vera* were collected from plants within the Prince Sattam bin Abdulaziz University campus and authenticated by a plant science expert; voucher specimens were not assigned. Standard laboratory strains of *Escherichia coli* and *Staphylococcus aureus* were procured from the Microbiology Laboratory, Prince Sattam bin Abdulaziz University, Al-Kharj, Saudi Arabia. Ethanol, Carbopol, glycerin, and methyl paraben were purchased from Loba Chemicals, India.

Preparation of green-synthesized silver nanoparticles

Silver nanoparticles (AgNPs) were synthesized using a green approach employing *Moringa oleifera (M. O.)* leaf extract as a natural reducing and stabilizing agent. Fresh leaves of MO were collected, washed, shade-dried, and ground into a fine powder. Dry powder was boiled with 100 ml (25 w/v) of distilled water for an hour below 100 °C, and the filtrate obtained served as the reducing extract [11]. MO extract containing flavonoids, polyphenols, and terpenoids, which effectively converted Ag^+ ions into metallic Ag nanoparticles. Upon mixing the 10 ml aqueous extract of MO with 90 ml of each solution of silver nitrate (1–5 mmol) under controlled conditions (250 rpm) of stirring and photocatalytic exposure, a gradual colour change was observed from pale greenish-yellow to brown and dark brown based on the concentration of silver nitrate, confirming nanoparticle formation (fig. 1). Preliminary optimization experiments were carried out using silver nitrate ($AgNO_3$) concentrations ranging from 1 to 5 mmol. Among the tested concentrations, AgNPs synthesized at 5 mmol $AgNO_3$ exhibited reproducible nanoparticle formation with stable colloidal characteristics, including nanoscale particle size, acceptable polydispersity, and a sufficiently negative zeta potential indicative of electrostatic stabilization. Lower $AgNO_3$ concentrations produced less consistent nanoparticle formation, whereas 5 mmol provided a higher yield of well-formed nanoparticles suitable for drug conjugation. Therefore, AgNPs synthesized using 5 mmol $AgNO_3$ were selected as the optimized formulation and used for subsequent adapalene conjugation and gel preparation. Increasing $AgNO_3$ concentration intensified this colour transition, accelerated reaction kinetics, and resulted in higher nucleation rates and superior AgNPs yield at higher molarities. The green-synthesized AgNPs were separated from the extract by centrifugation at 12,000 rpm for 15 min, yielding compact brown pellets, washed multiple times with milli-Q water and freeze-dried, producing stable AgNPs powder suitable for subsequent drug loading with ADN. The applied method of *Moringa oleifera* extract and synthesis of AgNPs provides an eco-friendly, efficient, and sustainable route for AgNPs green synthesis with $AgNO_3$.

Fig. 1: Color change indicating AgNP formation using *Moringa oleifera* extract

The concentration of green-synthesized silver nanoparticles (AgNPs) was determined after freeze-drying. A known volume of the freshly prepared AgNP suspension was lyophilized to obtain dry nanoparticle powder. The dried AgNPs mass was accurately weighed, and the nanoparticle concentration (mg/ml) was calculated based on the original suspension volume. This quantified AgNP concentration was subsequently used to calculate the drug-to-nanoparticle ratio (1:10, w/w) for adapalene conjugation.

Conjugation of adapalene onto AgNPs

Adapalene-AgNPs were prepared by a post-synthesis adsorption method. Since Adapalene (ADN) is poorly soluble in water (BCS Class II), an ADN saturated solution was prepared at 1 mg/ml (dissolved in ethanol–water 1:1) in an ethanol–water mixture to obtain a clear solution. The previously synthesised green AgNP suspension was then mixed with the ADN solution at a drug-to-nanoparticle ratio of 1:10 (w/w) and gently stirred for 2–4 h in the dark to prevent photo degradation of the ADN. During this incubation, ADN molecules adsorbed onto the surface of the green-synthesized AgNPs through hydrophobic interactions and possible π–π or van der Waals forces with phytochemical capping layers. The resulting dispersion was centrifuged at 12,000–15,000 rpm for 15–20 min to separate the ADN-conjugated AgNPs from the unbound ADN. The supernatant was collected for determining free ADN content, while the obtained pellet was washed with distilled water and resuspended to yield the final adapalene-conjugated silver nanoparticles (ADN–AgNPs) [12, 13]. Similar ADN-NPs ratios have been reported in nanoparticulate adapalene delivery systems intended for topical application, supporting the suitability of the selected formulation strategy [12].

Infusion of adapalene-conjugated silver nanoparticles in *Aloe vera* gel

Fresh aloe leaves were purchased from the supermarket; the leaves were cut from both ends, and the outer layer was peeled off. A blunt knife was used to scrape out the leaves, and aloe gel was blended. Collected gel was added with ADN–AgNPs (equivalent to 0.1%), methylparaben (0.1%), carbopol 934 (1.0% w/w), and glycerin (4% w/w). Triethanolamine was added to reach the pH (pH ≈ 5.5–6.5) and clear, smooth, stable gel consistency [14, 15].

Particle size, polydispersity index, and zeta potential analysis

The sample under investigation was dispersed into milli-Q water (1:700), agitated under water bath by ultrasonic waves using ultrasonic bath at room temperature for 3 min to disperse agglomerates, after which colloidal dispersion was filled into the disposable polystyrene cuvettes for size and PDI measurement whereas zeta potential was examined by filling the sample into the folded capillary cell (DTS1070). The average particle size, polydispersity index (PDI), and zeta potential of the synthesized Adapalene–AgNPs were determined using a Zetasizer Nano ZS (Malvern Instruments Ltd., Malvern, UK) based on Dynamic Light Scattering (DLS) and Electrophoretic Light Scattering techniques, respectively [16]. Stokes-Einstein equation (1) and Smoluchowski equation (2) were used for these analysis.

$$D_h = \frac{kT}{3\pi\eta D} \ldots (1)$$

Where k is the Boltzmann constant, T is the absolute temperature, η is the viscosity of the medium, and D is the translational diffusion constant.

$$\zeta = \frac{\mu_e \eta}{\epsilon} \ldots (2)$$

Where η is the viscosity and ∈ is the dielectric constant of the medium.

Fourier transform infrared (FTIR) spectroscopy analysis

The FT-IR spectrums of *Moringa oleifera* leaf extract and the green-synthesized AgNPs were taken using a Thermo Scientific Nicolet iD5 ATR diamond FT-IR spectrometer (Waltham, MA, USA**)** to identify functional groups involved in the reduction and stabilization of Silver(1+) cation. Dried samples of both the extract and AgNPs were directly placed on the center of ATR crystal, and spectra were recorded in the range of 4000–400 cm^{-1}. The recorded spectra were then compared to detect shifts or disappearance of peaks, confirming the participation of phytochemical constituents in AgNPs formation and stabilization [17].

X-ray diffraction (XRD) analysis

Green-synthesized silver nanoparticles were analyzed using X-ray diffraction (Rigaku MiniFlex 600, Tokyo, Japan). The dried AgNP powder was gently spread onto a clean glass slide to obtain a uniform sample layer and mounted on the sample holder. Diffraction measurements were performed using Cu Kα radiation (λ = 1.5406 Å) at an operating voltage of 40 kV and a current of 30 mA. The diffraction pattern was recorded over a 2θ range of 10°–80° at a scan rate of approximately 2°/min under ambient conditions. The obtained diffractograms were analyzed to identify diffraction features corresponding to metallic silver and phytochemical-associated crystalline components originating from the green synthesis process. Owing to the dominance of organic capping-related reflections, crystallite size estimation using the Debye–Scherrer equation was not applied to non-metallic peaks. The XRD analysis was therefore used primarily for qualitative assessment of crystallinity and phase identification [18].

Brunauer–emmett–teller surface area analysis

Determination of specific surface area of the synthesized nanoparticles by nitrogen adsorption–desorption using a Quantachrome Autosorb-iQ automated gas sorption analyzer (Quantachrome Instruments, USA). Dried sample under investigation, synthesized AgNPs (20 mg) was placed into a 9-mm analysis cell (without rod) and degassed under vacuum at 180 °C for 3.3 h to remove moisture and residual volatiles. After outgassing, the sample cell was transferred to the analysis port and cooled in a liquid nitrogen bath maintained at 77.35 K. High-purity nitrogen gas was used as the adsorbate, while helium gas was employed for void-volume calibration. Adsorption isotherms were collected over a relative pressure (P/P_0) range of 0.05–0.30, corresponding to the linear BET region. Automated gas dosing, equilibration, and data acquisition were performed using ASiQwin™ software (version 5.0). BET surface area was calculated from the monolayer adsorption volume (Vm) obtained from the slope and intercept of the BET plot, using a nitrogen molecular cross-sectional area of 16.2 $Å^2$ and a molecular weight of 28.013 g/mol. The specific surface area (m^2/g) was finally derived according to the standard BET equation [19]:

$$\text{Surface Area } (m^2/g) = \frac{V_m N_A \sigma}{22414} \ldots (3)$$

Where V_m is the monolayer capacity (cm^3/g), N_A is Avogadro's number, and σ is the cross-sectional area of nitrogen at STP.

Scanning electron microscopy (SEM)

The morphological features of the green-synthesized AgNPs were examined using Scanning Electron Microscopy (SEM) with an FEI Quanta 250 instrument (Hillsboro, USA). A small mass of the dried AgNPs was mounted on an aluminium stub using double-sided carbon adhesive tape to ensure proper fixation. The sample was sputter-coated with a thin layer of gold to induce enhanced electrical conductivity. The prepared specimen was then observed under the microscope at an accelerating voltage of 15–20 kV under high vacuum conditions. SEM micrographs were recorded at different magnifications and positions in the sample slab to evaluate the surface morphology and aggregation behavior of the green-synthesized AgNPs. The obtained images confirmed the formation of predominantly spherical and uniformly distributed nanoparticles [18].

Entrapment efficiency and drug loading of adapalene

A standard calibration curve was constructed for drug analysis in the given sample of green-synthesized AgNP dispersion. The unbound drug (supernatant) from the fabricated Adapalene–AgNP Conjugates dispersion was diluted and analyzed spectrophotometrically at 236 nm using a UV–Vis spectrophotometer against a blank [20]. The concentration of free adapalene was determined from the calibration curve, and the amount of unbound drug (mg) was calculated. The percentage entrapment efficiency was then calculated using the following equation (4):

$$EE\% = \frac{(\text{Total ADN added} - \text{Free ADN in supernatant})}{\text{Total ADN added}} X100 \text{ -------- } (4)$$

The mass of loaded drug (ADN) was obtained by subtracting the free drug (ADN) amount in the supernatant from the total amount of adapalene initially added. The percentage of drug loading was calculated by relating the mass of the loaded drug to the mass of the Adapalene–AgNP conjugates using equation (5):

$$DL\% = \frac{\text{Weight of loaded ADN (mg)}}{\text{Weight of dried ADN–AgNPs Conjugates (mg)}} X100 \text{ -------- (5)}$$

Physical evaluation of ADN–AgNP–integrated *Aloe vera* gel

Appearance and homogeneity

The prepared ADN–AgNP gel formulation filled in the beaker was visually examined under adequate light to assess clarity and uniformity. A small portion of the gel was spread on a glass slide using a sterile glass rod to evaluate its smoothness and dispersion consistency. The formulation was observed for the absence of visible lumps, aggregates, and phase separation, indicating proper homogeneity and stable dispersion of ADN-AgNPs-infused *Aloe vera* gel.

pH measurement

The pH of the adapalene–AgNP formulation was measured directly using a calibrated (Standard buffer solutions of pH 4.0, 7.0, and 9.2) digital pH meter. The pre-washed electrode was gently inserted into the gel and allowed to stabilize, after which the pH value was recorded (n=3).

Viscosity determination

The viscosity of the adapalene–AgNP infused gel was measured using a Brookfield viscometer**.** The sample was placed in the sample container, and the spindle was immersed without trapping air. The instrument was operated at room temperature (25±1 °C), and measurements were recorded at an appropriate spindle speed selected based on optimal torque range (typically 10–100 rpm). The viscosity value in centipoise (cP) was recorded once a constant reading was obtained [21].

Spreadability test

Weight equivalent to 1 g gel was placed centrally on a clean glass plate (10×10 cm) and covered with a second plate to form a thin film. A standard weight (e. g., 500 g) was placed on the top plate for 5 min at room temperature to allow spreading and expulsion of trapped air. The weight was removed, and the final spread area/diameter was measured in two perpendicular directions; the mean diameter was recorded.

Drug content uniformity

Drug content uniformity of the adapalene gel was assessed by transferring sampling (≈ 1.0 g) to a volumetric flask, protected from light, and extracted with methanol: phosphate buffer pH 7.4 (60:40, v/v) vortexing and sonication for 10–15 min to ensure complete drug dissolution; filtered (0.45 µm). After appropriate dilutions analyzed by UV–Vis at ~323 nm (Adapalene λmax) against the blank [22].

***In vitro* release study**

The ADN diffusion was studied by the Franz diffusion method, placing the sample equivalent to 50 mg of the under-study Adapalene–AgNPs on the pre-activated semipermeable (~12–14 kDa) dialysis membrane. The cell was filled with the 50 ml phosphate buffer (pH 7.4) maintained at 37±1 °C to simulate skin conditions, and the assembly was placed on the thermodynamically controlled magnetic stirrer plate. The medium was stirred in the circular laminar flow by continuously stirring at 50 rpm. At predetermined time intervals (e. g., 0.5, 1, 2, 4, and 6 h), 2 ml aliquots were withdrawn and immediately replaced with an equal volume of fresh buffer to maintain constant volume and sink conditions. To maintain sink conditions for the lipophilic drug adapalene, the receptor medium consisted of phosphate buffer (pH 7.4) supplemented with 1% (v/v) tween 80. The samples were filtered if required, and the concentration of adapalene in the release medium was quantified using a UV–Vis spectrophotometer at the predetermined λmax of adapalene ≈ 323 nm. The cumulative percentage of drug release was calculated and plotted as a function of time to obtain the release profile of adapalene from the AgNPs compared with the marketed formulation. Diffusion release data is fixed to release kinetics mathematical equation to find out the order of reaction and mechanism of drug release [23]. The dialysis membrane–based Franz diffusion setup was employed to evaluate *in vitro* drug release kinetics from the gel formulation and does not represent true transdermal or dermal permeation.

Stability study

The physicochemical parameter of the optimized ADN–AgNPs infused *Aloe vera* gel was evaluated according to ICH stability guidelines. The formulation was packed in airtight containers and stored under two conditions: room temperature storage at 25±2 °C/60±5% RH and accelerated storage at 40±2 °C/75±5% RH for a period of 90 d**.** Samples were withdrawn at predetermined intervals (0, 30, 60, and 90 d) and evaluated for appearance and drug content.

Although stability assessment was conducted under ICH accelerated conditions (40±2 °C/75±5% RH) based on visual appearance, pH, drug content, and *in vitro* release behavior, time-dependent changes in polydispersity index, zeta potential, and viscosity were not evaluated. This limitation is acknowledged, as the present study primarily focused on formulation feasibility and performance rather than long-term colloidal and rheological stability.

Antimicrobial activity

The antibacterial activity of the developed adapalene-infused AgNPs gel was evaluated against *Escherichia coli* and *Staphylococcus aureus*. The disc diffusion method was employed for screening antibacterial efficacy. The ditch plate technique was used to test the sample by placing it on nutrient agar plates inoculated with the test microorganisms. A commercial adapalene gel was used as the control. The plates were incubated at 37 °C for 24 h, after which the zones of inhibition (mm) around each bore were measured using a digital calliper. All experiments were performed in triplicate, and results were expressed as mean±standard deviation [24].

RESULTS AND DISCUSSION

Particle size, polydispersity index, and zeta potential analysis

Particle analysis was done by the Dynamic Light Scattering (DLS) method, the optimized ADN-AgNPs conjugate showed a Z-average particle size, PDI and Zeta potential of (228.5 nm), (0.502), (−24.5 mV) indicating formation of nanosized particles (fig. 2), moderate broad polydispersity and acceptable colloidal stability; the negative charge arises from plant-derived phytochemicals adsorbed onto the nanoparticle surface, providing electrostatic repulsion that prevents immediate aggregation. These results correlate well with previously reported size range corresponds well with green-mediated AgNPs previously synthesized using *Moringa oleifera* and other phytochemical-rich extracts, typically reported within 80–250 nm [25]. Although the PDI value of 0.502 reflects moderately broad polydispersity, such behavior is commonly observed in phyto-mediated green synthesis due to variable nucleation and surface capping by multiple phytoconstituents. Additional broadening of size distribution may also occur during drug conjugation as a result of partial nanoparticle aggregation or surface restructuring.

It should be noted that while a PDI of 0.502 indicates moderate polydispersity, such distribution is acceptable for topical, phyto-mediated nanoparticle systems where follicular deposition and surface interaction dominate drug performance; however, this level of heterogeneity would be unsuitable for parenteral or systemic delivery applications requiring narrow size distributions.

The particle size below 300 nm is particularly relevant for topical delivery, as nanoparticles in this range preferentially accumulate within pilosebaceous units, enhancing localized drug deposition. Although the observed PDI indicates a moderately broad size distribution, similar values have been reported for phyto-mediated silver nanoparticles due to the heterogeneous composition of plant extracts [7, 27]. Importantly, the stable negative zeta potential (−24.5 mV) suggests sufficient electrostatic repulsion to maintain colloidal stability, mitigating concerns related to polydispersity for topical application [18].

The optimized AgNPs selected for drug conjugation were synthesized using 5 mmol $AgNO_3$, as this concentration provided the best balance between nanoscale size, colloidal stability, and reproducibility compared with lower precursor concentrations.

Fourier transform infrared (FTIR) spectroscopy analysis

The FTIR spectrum of pure Adapalene (fig. 3a) displayed characteristic absorption peaks at 3050–3100 cm^{-1} (C–H stretch in

aldehyde and ketone) typical of the substituted naphthalene and benzene rings, 2920–2950 cm^{-1} (aliphatic C–H stretching) arising from the propionate side chain, sharp absorption around 1680–1700 cm^{-1} (C = O stretch) one of the key identifying peaks of Adapalene,1500 cm^{-1} (C = C stretch) confirming the presence of multiple aromatic rings, 1300 cm^{-1} (–C–O stretch) of carboxylate moiety, 1150 cm^{-1}(C–N stretching) vibrations of the amine-containing aromatic moiety, and 700 and 900 cm^{-1} (aromatic C–H out-of-plane bending). Together, these peaks confirm the presence of all the expected functional groups of adapalene, these fingerprint region peaks confirm that adapalene retained its chemical structure following nanoparticle conjugation. Similar downshifts in carbonyl and aromatic peaks have been documented during the conjugation of hydrophobic drugs onto phyto-capped AgNPs, indicating partial coordination of oxygen-containing functional groups with the nanoparticle surface or phytochemical capping layer [26].

The FTIR spectrum of the adapalene–*Moringa oleifera*–mediated AgNP conjugate exhibited moderate shifts, band broadening, and changes in intensity relative to pure adapalene, suggesting an interaction between the drug and the phytochemicals capped nanoparticle surface. Notably, the absence of new absorption bands and the lack of pronounced peak shifts indicate that strong covalent or coordination bonding between silver and adapalene functional groups is unlikely.

The observed broadening of aromatic C–H and C=C bands and minor downshifts in carbonyl and C–O stretching regions are consistent with non-covalent interactions, such as hydrophobic association, π–π stacking, hydrogen bonding, and van der Waals forces, facilitated by the phytochemical capping layer derived from *Moringa oleifera*. Importantly, the retention of characteristic adapalene bands suggests surface association rather than chemical modification of the drug molecule. FTIR spectroscopy provides qualitative insight into molecular interactions; therefore, the proposed conjugation mechanism is inferred rather than conclusively established. The data support a phytochemical-assisted, non-covalent association of adapalene with AgNPs rather than direct metal–ligand coordination (fig. 3b). This behavior is consistent with previously reported phytochemical-assisted conjugation mechanisms, where drug association occurs primarily through hydrogen bonding and π–π interactions mediated by plant-derived polyphenols [26, 27]. Further confirmation of the interaction mechanism would require surface-sensitive techniques such as X-ray photoelectron spectroscopy (XPS) or competitive binding studies, which were beyond the scope of the present work.

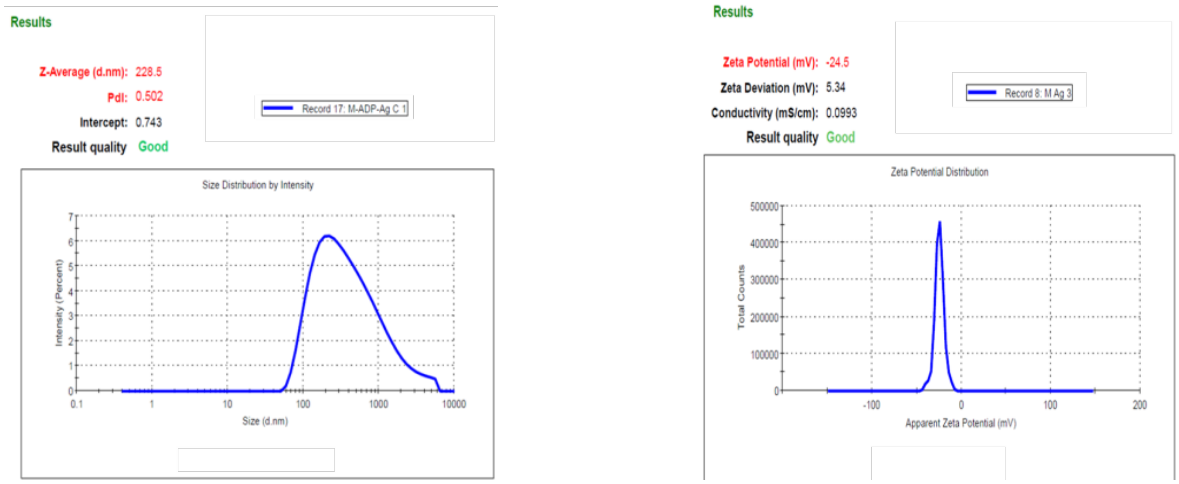

a **b**

Fig. 2: Particle size distribution, PDI (a), and zeta potential (b)of optimized ADN–AgNP conjugates

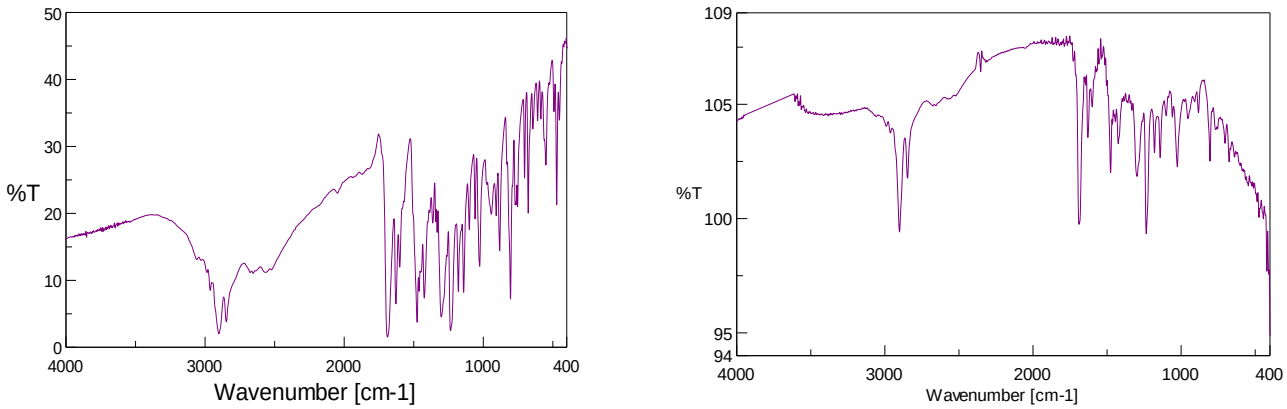

ADN – Pure drug (a) **ADN–AgNPs (b)**

Fig. 3: FTIR spectrum of ADN – Pure drug and ADN-AgNPs conjugate

X-ray diffraction (XRD) analysis

The XRD pattern of the ADN–AgNPs revealed a semi-crystalline profile with multiple diffraction features (fig. 4). A prominent intense peak was observed at 2θ ≈ 22.16°, which does not correspond to face-centered cubic (fcc) metallic silver and is therefore attributed to crystalline or semi-crystalline organic components arising from the *Moringa oleifera* phytochemical

capping layer and associated biomatrix residues. Similar organic-associated diffraction peaks in the 20–25° range have been widely reported for plant-mediated silver nanoparticles.

In addition, weak and broadened reflections were observed in the region of 2θ ≈ 35–40°, which may be assigned to the (111) plane of fcc silver, consistent with JCPDS card no. 04-0783. The relatively low intensity and broad nature of these reflections can be attributed to the dominance of the organic capping layer, small crystallite domains, and partial masking of metallic silver peaks by phytochemical constituents. Crystallite size estimation using the Scherrer equation was not applied due to peak overlap and phytochemical interference; therefore, XRD was used only for phase confirmation.

Owing to the non-metallic origin of the dominant 22.16° peak, crystallite size estimation based on this reflection was deemed inappropriate. Instead, the XRD data were interpreted qualitatively to confirm the presence of nanocrystalline silver embedded within a bio-organic matrix rather than relying on Scherrer-based size calculation from organic reflections. This diffraction behavior is characteristic of green-synthesized, phyto-capped AgNPs reported in earlier studies [27].

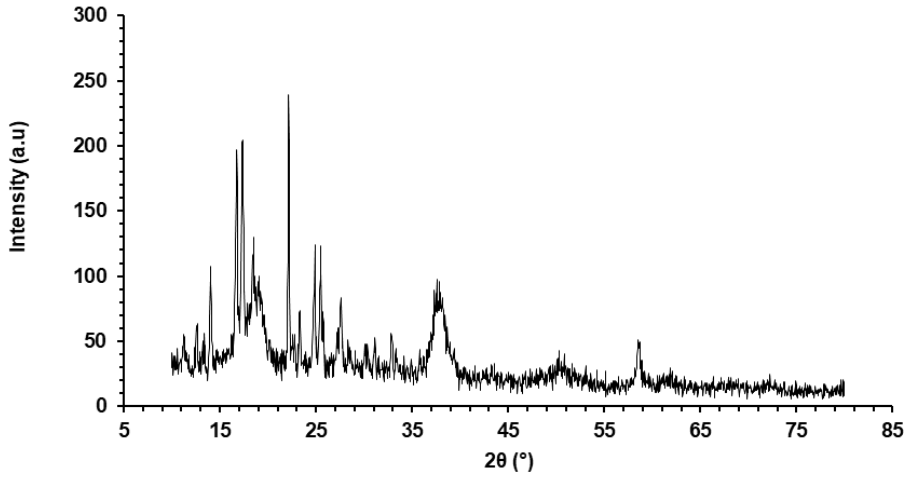

Fig. 4: XRD pattern of ADN-AgNPs conjugate showing the main diffraction peak

Brunauer–emmett–teller surface area analysis

BET analysis confirmed the formation of high-surface-area nanoparticles, with the BET model applied over the linear P/P_0 range of 0.05–0.30. The BET plot exhibited excellent linearity (r^2 0.995802), validating the reliability of the fit. The calculated BET slope (38.391 1/g) and intercept (1.053 1/g) yielded a BET constant (C = 37.465), indicative of moderate adsorbate–adsorbent interactions typical of well-dispersed nanostructured systems. From these parameters (table 1), the specific surface area was determined to be 88.293 m^2/g, reflecting the presence of small, highly reactive particles with extensive accessible surface. The nitrogen adsorption isotherm (fig. 5). Further supports the physisorption-driven uptake characteristic of mesoporous or nanostructured materials. The high surface area is consistent with efficient green synthesis using *Moringa oleifera* extract, which promotes rapid nucleation and limits particle agglomeration. Such a large surface-to-volume ratio provides enhanced drug loading (ADN) potential and improved interaction with biological membranes, contributing to the superior performance expected from adapalene-loaded AgNP topical formulations.

The BET surface area of 88.293 m^2/g represents large accessible surface, which can directly involve to accommodate ADN, therefore exhibits improved drug loading of (48.92%). This relationship between surface area and loading has been widely noted for nano-carriers, where higher specific surface area increases adsorption-driven drug incorporation.

Similar correlations between increased surface area and enhanced drug loading have been reported for nanostructured silver carriers and polymeric nanosponges [16, 18], supporting the efficiency of the present nanocarrier system.

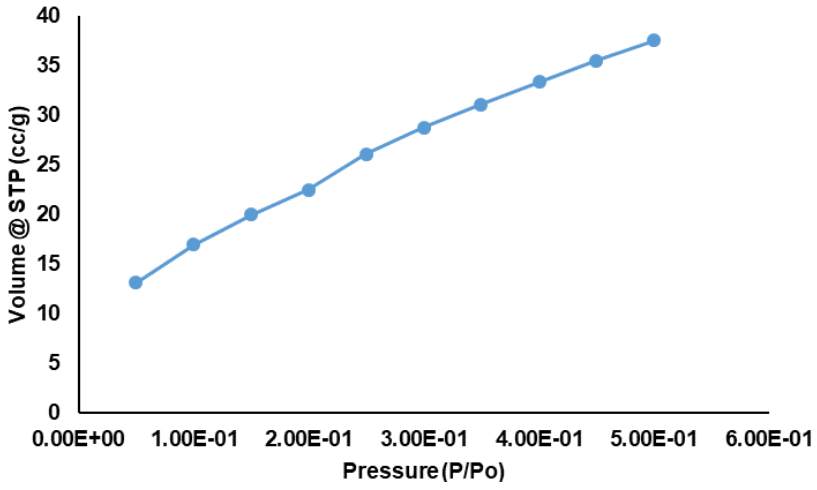

Fig. 5: Nitrogen adsorption isotherm at 77 K

Table 1: BET surface area parameters obtained from nitrogen adsorption analysis

Parameter	Value
Slope	38.391 1/g
Intercept	1.053 1/g
Correlation Coefficient (r)	0.995802
BET Constant (C)	37.465
Specific Surface Area (BET Surface Area)	88.293 m^2/g

BET surface area was calculated from the linearized BET plot (P/P_0 = 0.05–0.30). The BET constant (C) represents the interaction strength between nitrogen molecules and the nanoparticle surface. The slope and intercept were derived from the linear BET equation and used for surface area determination.

Scanning electron microscopy (SEM)

Green synthesized AgNPs conjugated with the drug (ADN) exhibit the cluster of particles of quasi-spherical shape. The observed particle clustering is attributed to phytoconstituents from *Moringa oleifera* extract that act as natural reducing and capping agents. These biomolecules stabilize the particles but also promote secondary agglomeration during drying, giving rise to the granular, cauliflower-like structures seen in the image. The absence of rod-shaped or faceted crystal structures confirms that the synthesis pathway successfully produced isotropic metallic nanoparticles. AgNPs with nanoscale, confirming the effectiveness of the green synthesis method. SEM morphology confirms effective reduction, capping, and stabilization of AgNPs by Moringa extract (fig. 6), consistent with the mechanistic understanding outlined by *Eker et al.*, and supports the suitability of these nanoparticles for topical drug delivery, where spherical geometry improves topical drug delivery and enhances antimicrobial performance [28].

The cauliflower-like aggregation observed in SEM images represents the dried state of the nanoparticles following solvent evaporation and sample preparation under vacuum conditions. In the final formulation, the ADN–AgNPs are dispersed within a hydrated *Aloe vera*–based gel matrix, where such dry-state clustering is may partially redisperse. Upon hydration, the phyto-capped AgNP aggregates are expected to partially redisperse due to electrostatic repulsion (ζP = −24.5 mV) and steric stabilization provided by the polymeric gel network. Similar behavior has been reported for nanoparticle systems where apparent aggregation in SEM does not reflect dispersion under hydrated or in situ conditions. Importantly, incorporation of clustered nanostructures within a viscous gel may contribute to controlled drug diffusion by increasing the tortuosity of the diffusion pathway, thereby supporting sustained release without compromising topical applicability. The SEM micrographs revealed quasi-spherical nanoparticles with localized aggregation, which is commonly observed in green-synthesized systems due to phytochemical capping and partial drying-induced particle association. Such aggregation may partially redisperse upon rehydration, although this interpretation is inferred from formulation behavior and was not directly evaluated in the present study. The observed morphology remains suitable for topical application. Therefore, SEM-observed aggregation should be interpreted as a preparation-induced phenomenon rather than an indicator of in-gel dispersion behavior.

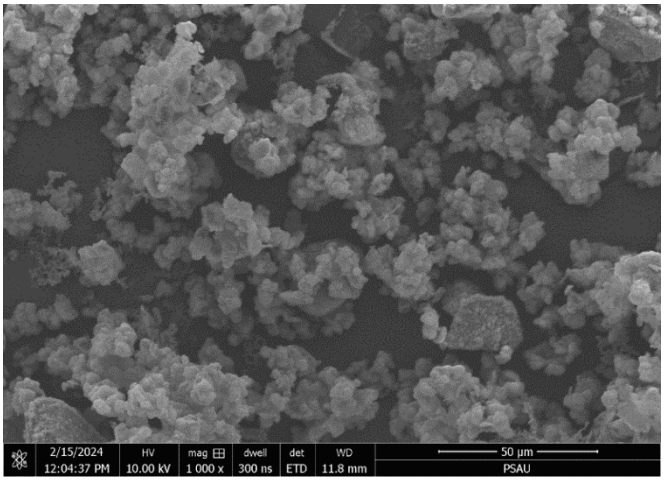

Fig. 6: SEM image showing the surface morphology of the Adapalene–AgNP conjugates

Entrapment efficiency and drug loading of adapalene

The quantification of the loaded ADN with the green synthesized AgNPs was performed with the calibration curve equation that showed a strong linear relationship between absorbance and concentration with the regression equation (A: 0.0121; C – 0.0663) and an excellent correlation coefficient ($R^2 \approx 0.999$); these parameters were used to calculate the concentration of the test samples. Entrapment efficiency, calculated using equation 2 from the supernatant, unbounded ADN, was found to be 2.155 mg, indicating 97.84 mg was entrapped within the AgNPs, corresponding to remarkably high entrapment efficiency (EE% = 97.85%), suggesting excellent drug–nanoparticle interaction. The strong binding can be attributed to hydrophobic forces, π–π interactions, and the presence of phytochemicals (flavonoids, polyphenols, and terpenoids) from *Moringa oleifera* extract, which act as natural capping and stabilizing agents. Furthermore, the calculation of DL was also performed using equation 3, taking 200 mg of the dried mass of adapalene–AgNP conjugates exhibiting drug loading of 48.92%, signifying half of the nanoparticle mass consisted of active drug. The ADN-AgNPs final conjugate contained 48.92% w/w adapalene and 51.08% w/w silver nanoparticles**.** Such higher loading is highly beneficial for the topical therapy, wherein the epidermis acts as a barrier. The high DL% observed is consistent with the large BET surface area, which increases the available adsorption/interface sites for drug association. Drug conjugated in AgNPs with minimal excipient burden facilitates the drug release with a mol. wt of ADN (412.52 g/mol) in the nanorange for effective topical delivery of adapalene.

The drug-to-nanoparticle ratio of 1:10 (w/w) was selected based on prior reports on adapalene-loaded nanocarriers, where similar drug-to-carrier ratios (1:5 to 1:15 w/w) were shown to provide high

entrapment efficiency while maintaining colloidal stability and controlled topical release. In particular, adapalene-loaded polymeric and nanoparticulate systems have commonly employed comparable ratios to achieve effective epidermal localization without drug crystallization or carrier saturation [12, 26]. The selected ratio in the present study ensured high drug loading (48.92%) with excellent entrapment efficiency (97.85%) while preserving nanoparticle stability, making it suitable for topical delivery.

Physical evaluation of ADN–AgNP–integrated *Aloe vera* gel

The ADN–AgNP topical *Aloe vera* gel showed a smooth, lump-free appearance with no phase separation, confirming proper homogeneity and uniform stable nanoparticle gel dispersion.

The pH of the ADN–AgNP gel was successfully adjusted to a dermal range of 5.5–6.5 using triethanolamine. The sample showed the pH (6.06±0.2), confirming good formulation, skin compatibility, stability and suitability for topical application. The viscosity of the ADN–AgNP gel was 12,000 cP, measured using spindle no. 64 at 20 rpm, indicating suitable consistency for topical application. This viscosity ensures smooth spreadability, good structural integrity, and stable retention on the skin. The result also confirms proper polymer hydration and uniform dispersion of the adapalene–AgNPs without phase separation, indicating a stable and well-formulated gel.

The ADN–AgNP gel exhibited excellent drug content uniformity, with individual samples showing values between 95.65%and 98.54%, and a mean drug content of 97.11±1.18%. These values fall well within the pharmacopeial acceptance limits of 90–110% of the labelled claim**,** indicating accurate drug loading and consistent distribution of adapalene throughout the gel matrix.

The spreadability study of the ADN–AgNP gel demonstrated that the formulation possessed excellent extensibility and ease of application. Using 1 g of gel compressed under a 500 g weight for 5 min, the formulation achieved a mean spread diameter of 6.4±0.2 cm, indicating smooth and uniform spreading.

***In vitro* release study**

Comparative diffusion studies reflect progressive increase in the diffusion, followed by sustained release of drug. As the drug is conjugated with the AgNPs, initial burst effect was observed with 11.52±0.66% at 30 min time interval due to adsorption of the drug on the nanoparticle surface, that get increased to 97.99±1.89% at about 6 h compared to 43.30±3.4% for marketed formulation, representing a 2.26-fold increase in adapalene release compared with the marketed formulation. The superior release performance of the ADN–AgNP gel can be attributed to the nanoscale size of the AgNP carrier, which increases surface area and improves the dissolution and diffusion characteristics of poorly water-soluble adapalene. Diffusion-mediated release could be attributed the gel matrix, wherein the marketed formulation showed diffusion comparatively limited diffusion due to its denser polymeric base, larger particle size, and reduced permeability. The inclusion of tween 80 in the receptor phase ensured adequate solubilization of adapalene, thereby maintaining sink conditions throughout the release study. ADN–AgNP gel significantly enhanced cumulative drug release, indicating its strong potential as an improved topical delivery system for achieving faster therapeutic action in acne treatment. Similar release behavior has been reported for nanoparticle-loaded topical gels, where polymer hydration plays a critical role in modulating drug release [21, 23].

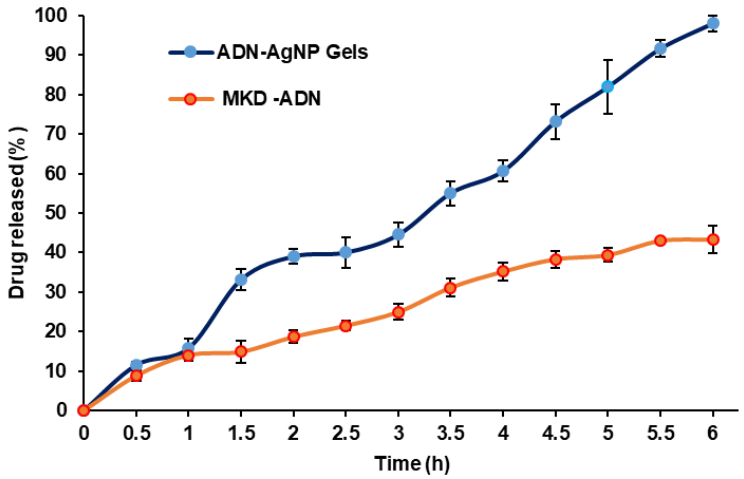

Fig. 7: *In vitro* drug release profiles of ADN–AgNP gels and MKD AND

Table 2: Kinetic modeling of the *in vitro* drug release profile of ADN–AgNP gel

Model	Regression equation	R^2	Release exponent (n)
Zero-order	(Q = 15.726t+2.3889)	0.9863	–
First-order	Log of (100 − Q) = −0.0178t+1.5812	0.0040	–
Higuchi	$Q = 41.407\ t^{1/2} - 16.308$	0.9161	–
Korsmeyer–Peppas	Log of $(Mt/M\infty)$ = 0.8713 log(t) − 0.7162	0.8892	0.8713

For the Korsmeyer–Peppas model, n values between 0.45 and 0.89 indicate anomalous (non-Fickian) transport involving both diffusion and polymer relaxation, while n ≥ 0.89 corresponds to case-II transport.

The release kinetics data of (table 1) described, ADN-AgNPs gel best demonstrated the zero-order model (R^2 = 0.9863), indicating a constant and diffusion-mediated release independent of drug concentration within 6 h. The Higuchi model also showed strong linearity (R^2 = 0.9161), confirming that Fickian diffusion plays a major role in drug transport through the gel matrix. However, the first-order model showed very poor correlation (R^2 = 0.0040), indicating that drug release is not concentration-dependent.

The Korsmeyer–Peppas model yielded a release exponent (n) value of approximately 0.87 (R^2 = 0.8892), which is characteristic of anomalous (non-Fickian) transport rather than true case-II or super case-II behavior. In hydrophilic polymeric systems such as carbopol 934 gels, n values between 0.45 and 0.89 indicate a release mechanism governed by both Fickian diffusion and polymer chain relaxation/swelling. In the present formulation, adapalene release is therefore controlled by diffusion from the ADN–AgNPs in

combination with swelling and relaxation of the carbopol–*Aloe vera* gel matrix. The incorporation of nanosized AgNPs further modulates the gel microstructure and diffusion pathways, contributing to controlled and sustained drug release. These findings are consistent with previously reported nanoparticle-loaded carbopol gel systems designed for topical delivery.

It is important to emphasize that the *in vitro* release study was performed using a dialysis membrane (12–14 kDa MWCO), which evaluates drug release from the gel matrix rather than true skin permeation. Dialysis membranes lack the complex lipid architecture and barrier properties of the stratum corneum and may therefore overestimate drug availability. Accordingly, all findings from this study should be interpreted as *in vitro* release kinetics rather than transdermal or dermal delivery performance. Future investigations employing ex-vivo skin models or synthetic skin-mimicking membranes such as Strat-M® are warranted to more accurately predict *in vivo* dermal permeation.

Stability study

The ADN–AgNP gel remained physically stable over the 90-day study period, with no observable changes in color, texture, or phase separation. Drug content ranged from 94.78–95.81%**,** with an average value of 95.13±0.4%**,** which is within acceptable pharmacopeia limits (90–110%) under all storage conditions. No visually detectable changes in gel consistency were observed during storage, indicating preserved rheological integrity. Although minor variations in particle size distribution and surface charge may occur over time, the formulation retained acceptable colloidal stability suitable for topical application. These findings confirm good physical and chemical stability of the formulation for short-to intermediate-term storage.

The absence of longitudinal measurements of polydispersity index, zeta potential, and viscosity represents a limitation of the present work. These parameters will be systematically investigated in future studies to provide a comprehensive understanding of long-term colloidal and rheological stability of the topical gel formulation.

Antimicrobial activity

The Antibacterial study of prepared ADN-AgNPs conjugated infused gel shows stronger antibacterial effects. Moringa extract alone shows very little antibacterial activity against E. coli (4±0.68 mm) and moderate activity against S. aureus (13±0.27 mm), which shows that it has some antibacterial properties. It's in line with previously reported inhibition zones of methanolic *M. oleifera* leaf extracts composed of flavonoids and phenolic acids such as quercetin and chlorogenic acid. El-Sherbiny *et al.* studied a similar study against the foodborne pathogens, including *E. coli* and *S. aureus* [29, 30]. The marketed product reflects strong, broad-spectrum activity with 16±0.17 mm zones for both organisms, confirming the well-known bactericidal effect. The ADN–AgNPs gel showed substantial inhibition—13±0.36 mm for *E. coli* and 16±0.14 mm for *S. aureus*—indicating that conjugated AgNPs within the adapalene–*Aloe vera* gel matrix demonstrate significant antimicrobial potency. Efficient antimicrobial effects of the ADN–AgNP topical gel could be due to the multifunctional antimicrobial effect of AgNPs releasing Ag^+ ions that disrupt bacterial cell membranes, penetrate within cells, and generate reactive oxygen species (ROS) that damage essential biomolecules (proteins and DNA), resulting in rapid bactericidal action. adapalene acts by decreasing follicular occlusion, limiting microbial colonisation, and exercising anti-inflammatory effects, while its conjugation with nanoscale AgNPs improves drug availability at the infection site [31]. Moreover, *Moringa oleifera* phytochemicals, such as quercetin, gallic acid, and rutin, stabilise AgNPs and provide additional membrane-disruptive, enzyme-inhibitory, and ROS-modulating actions. Together, these components create a potent, multi-targeted antibacterial system effective against both Gram-positive and Gram-negative bacteria. Therefore, the developed topical gel could be considered an effective and efficient medication for young women suffering from acne during their teenage years. The observed antimicrobial activity reflects the combined effects of silver nanoparticles, adapalene, and bioactive phytochemicals from *Moringa oleifera*. Comparable inhibition zones have been reported for green-synthesized AgNPs stabilized with plant extracts, supporting the multifunctional antimicrobial potential of the formulation [6, 11, 18].

Although the formulated adapalene-conjugated AgNPs gel demonstrated pronounced antimicrobial activity against both Gram-positive and Gram-negative organisms, a formulation containing only green-synthesized AgNPs without adapalene was not included as a separate control. Therefore, the relative individual contributions of adapalene and AgNPs cannot be quantitatively distinguished, and the observed activity should be interpreted as a combined or multifunctional antimicrobial effect rather than definitive synergism. Future studies will include appropriate single-component controls to enable formal synergy assessment.

The observed antimicrobial activity represents a combined or multifunctional effect arising from the intrinsic antimicrobial properties of silver nanoparticles, adapalene, and phytochemical capping agents, rather than a demonstrated synergistic interaction.

CONCLUSION

This study demonstrates that a green-synthesized adapalene-conjugated silver nanoparticle system can be successfully developed and infused into an *Aloe vera*-based topical gel as a new way to treat acne. Using the reducing and stabilizing properties of *Moringa oleifera* phytochemicals, researchers made stable nanosilver carriers that could hold drugs, and had a large effective surface area with reduced particle size that made them suitable to deliver ADN deeper into the skin. The formulated ADN–AgNPs gel had better release, longer-lasting drug release, anddemonstrated effective combined antimicrobial activity suitable for topical acne management. This shows how adapalene, nanosilver, and botanical components work together. This study demonstrates that plant-based nanomedicine may offer advantages over conventional topical acne therapies. It also lays the groundwork for future preclinical and clinical testing to move this eco-friendly nanogel closer to being used as a treatment.

ACKNOWLEDGEMENT

The authors extend their appreciation to Prince Sattam bin Abdulaziz University for funding this research work through the project number (PSAU/2023/03/27618).

AUTHORS CONTRIBUTIONS

Farhat Fatima contributed to conceptualization, methodology, experimental investigation, data curation, formal analysis, and original draft preparation. Asma B. Omer provided experimental support and data interpretation. Ahmed Al Saqr contributed resources, supervision, project administration, and critical review of the manuscript. Mohammed Muqtader Ahmed contributed to conceptualization, supervision, data analysis, manuscript review and editing.

CONFLICT OF INTERESTS

Declared none

REFERENCES

1. Alanazi MS, Hammad SM, Mohamed AE. Prevalence and psychological impact of acne vulgaris among female secondary school students in Arar city, Saudi Arabia, in 2018. Electron Physician. 2018;10(8):7224-9. doi: 10.19082/7224, PMID 30214705.
2. Piskin S, Uzunali E. A review of the use of adapalene for the treatment of acne vulgaris. Ther Clin Risk Manag. 2007;3(4):621-4. PMID 18472984.
3. Raina N, Rani R, Thakur VK, Gupta M. New insights in topical drug delivery for skin disorders: from a nanotechnological perspective. ACS Omega. 2023;8(22):19145-67. doi: 10.1021/acsomega.2c08016, PMID 37305231.
4. Rusu A, Tanase C, Pascu GA, Todoran N. Recent advances regarding the therapeutic potential of adapalene. Pharmaceuticals (Basel). 2020;13(9):217. doi: 10.3390/ph13090217, PMID 32872149.
5. Yu YQ, Yang X, Wu XF, Fan YB. Enhancing permeation of drug molecules across the skin via delivery in nanocarriers: novel

strategies for effective transdermal applications. Front Bioeng Biotechnol. 2021;9:646554. doi: 10.3389/fbioe.2021.646554, PMID 33855015.

6. Casals E, Gusta MF, Bastus N, Rello J, Puntes V. Silver nanoparticles and antibiotics: a promising synergistic approach to multidrug-resistant infections. Microorganisms. 2025;13(4):952. doi: 10.3390/microorganisms13040952, PMID 40284788.
7. Fahim M, Shahzaib A, Nishat N, Jahan A, Bhat TA, Inam A. Green synthesis of silver nanoparticles: a comprehensive review of methods influencing factors and applications. JCIS Open. 2024;16:100125. doi: 10.1016/j.jciso.2024.100125.
8. Ahmadi F, Lackner M. Green synthesis of silver nanoparticles from Cannabis sativa: properties synthesis mechanistic aspects and applications. Chem Engineering. 2024;8(4):64. doi: 10.3390/chemengineering8040064.
9. Athiya Afreena M, Ranjani S, Hemalatha S. Probiotic bacteria Bacillus licheniformis mediated sustainable green synthesis of nanoparticles and its multifaceted mechanisms to control dermal pathogens. Mater Chem Phys. 2025;345:131261. doi: 10.1016/j.matchemphys.2025.131261.
10. Hekmatpou D, Mehrabi F, Rahzani K, Aminiyan A. The effect of Aloe vera clinical trials on prevention and healing of skin wound: a systematic review. Iran J Med Sci. 2019;44(1):1-9. PMID 30666070.
11. Coelho N, Jacinto JP, Silva R, Soares JC, Pereira AS, Tavares P. Green synthesis and antibacterial activity of silver nanoparticles obtained from *Moringa oleifera* seed cake. Coatings. 2023;13(8):1439. doi: 10.3390/coatings13081439.
12. Bhalekar M, Upadhaya P, Madgulkar A. Formulation and evaluation of adapalene-loaded nanoparticulates for epidermal localization. Drug Deliv Transl Res. 2015;5(6):585-95. doi: 10.1007/s13346-015-0261-z, PMID 26483036.
13. Anwar N, Khan A, Shah M, Walsh JJ, Saleem S, Anwar Z. Hybridization of green synthesized silver nanoparticles with poly(ethylene glycol) methacrylate and their biomedical applications. Peer J. 2022;10:e12540. doi: 10.7717/peerj.12540, PMID 35111388.
14. Tippayawat P, Phromviyo N, Boueroy P, Chompoosor A. Green synthesis of silver nanoparticles in *Aloe vera* plant extract prepared by a hydrothermal method and their synergistic antibacterial activity. Peer J. 2016;4:e2589. doi: 10.7717/peerj.2589, PMID 27781173.
15. Surjushe A, Vasani R, Saple DG. *Aloe vera*: a short review. Indian J Dermatol. 2008;53(4):163-6. doi: 10.4103/0019-5154.44785, PMID 19882025.
16. Fatima F, Anwer MK. Development and characterization of ibrutinib-loaded ethylcellulose-based nanosponges: cytotoxicity assay against MCF-7 cell lines. Appl Sci. 2023;13(8):4984. doi: 10.3390/app13084984.
17. Pasieczna Patkowska S, Cichy M, Flieger J. Application of Fourier transform infrared (FTIR) spectroscopy in characterization of green synthesized nanoparticles. Molecules. 2025;30(3):684. doi: 10.3390/molecules30030684, PMID 39942788.
18. Asif M, Yasmin R, Asif R, Ambreen A, Mustafa M, Umbreen S. Green synthesis of silver nanoparticles (AgNPs), structural characterization and their antibacterial potential. Dose Response. 2022;20(1):15593258221088709. doi: 10.1177/15593258221088709, PMID 35592270.
19. Priyadarshini V, Tharini K, Kalaimagal G, Alvin Kalicharan A, Subhashini B, Rathinavelu A. Green engineered silver (Ag NPs) nanoparticles enable for thermal optical behavior and catalytic elimination of organic pollutants. Results Surf Interfaces. 2025;20:100593. doi: 10.1016/j.rsurfi.2025.100593.
20. Vichare VS, Handargule PV. Simultaneous estimation of dapsone and adapalene in gel formulation by UV-spectroscopy. Int J Pharm Sci Res. 2020;11(12):6179-83.
21. Dantas MG, Reis SA, Damasceno CM, Rolim LA, Rolim Neto PJ, Carvalho FO. Development and evaluation of stability of a gel formulation containing the monoterpene borneol. Scientific World Journal. 2016;2016:7394685. doi: 10.1155/2016/7394685, PMID 27247965.
22. Boateng J, Khan S. Composite HPMC-gelatin films loaded with Cameroonian and Manuka honeys show antibacterial and functional wound dressing properties. Gels. 2025;11(7):557. doi: 10.3390/gels11070557, PMID 40710718.
23. Salamanca CH, Barrera Ocampo A, Lasso JC, Camacho N, Yarce CJ. Franz diffusion cell approach for pre-formulation characterisation of ketoprofen semi-solid dosage forms. Pharmaceutics. 2018;10(3):148. doi: 10.3390/pharmaceutics10030148, PMID 30189634.
24. Cunha FA, Maia KR, Mallman EJ, Cunha MD, Maciel AA, Souza IP. Silver nanoparticles-disk diffusion test against Escherichia coli isolates. Rev Inst Med Trop Sao Paulo. 2016;58:73. doi: 10.1590/S1678-9946201658073, PMID 27680178.
25. Mohammed GM, Hawar SN. Green biosynthesis of silver nanoparticles from *Moringa oleifera* leaves and its antimicrobial and cytotoxicity activities. Int J Biomater. 2022;2022:4136641. doi: 10.1155/2022/4136641, PMID 36193175.
26. Nadal JM, Dos Anjos Camargo G, Novatski A, Macenhan WR, Dias DT, Barboza FM. Adapalene-loaded poly(ε-caprolactone) microparticles: physicochemical characterization and *in vitro* penetration by photoacoustic spectroscopy. PLOS One. 2019;14(3):e0213625. doi: 10.1371/journal.pone.0213625, PMID 30897170.
27. Iravani S. Green synthesis of metal nanoparticles using plants. Green Chem. 2011;13(10):2638-50. doi: 10.1039/C1GC15386B.
28. Eker F, Akdasci E, Duman H, Bechelany M, Karav S. Green synthesis of silver nanoparticles using plant extracts: a comprehensive review of physicochemical properties and multifunctional applications. Int J Mol Sci. 2025;26(13):6222. doi: 10.3390/ijms26136222, PMID 40650001.
29. El-Sherbiny GM, Alluqmani AJ, Elsehemy IA, Kalaba MH. Antibacterial antioxidant, cytotoxicity and phytochemical screening of *Moringa oleifera* leaves. Sci Rep. 2024;14(1):30485. doi: 10.1038/s41598-024-80700-y, PMID 39681592.
30. Bagheri R, Rashidlamir A, Ashtary Larky D, Wong A, Grubbs B, Motevalli MS. Effects of green tea extract supplementation and endurance training on irisin, pro-inflammatory cytokines, and adiponectin concentrations in overweight middle-aged men. Eur J Appl Physiol. 2020;120(4):915-23. doi: 10.1007/s00421-020-04332-6, PMID 32095935.
31. Dutta S, Mohapatra P, Rath K, Kar DM, Priyanka Birla, Manish D Shind. Pharmacy students' knowledge, attitude and practice concerning diabetes and its long-term complications-a cross-sectional study. Asian J Pharm Clin Res. 2025;18(6):228-33. doi: 10.22159/ajpcr.2025v18i6.54631.